Synthesis, Structure and Properties of the System B_2O_3/Al_2O_3

T. R. KARPOVA, E. A. BULUCHEVSKII, A. V. LAVRENOV, N. N. LEONTYEVA, M. V. TRENIKHIN, T. I. GULYAEVA and V. P. TALZI

Institute of Hydrocarbons Processing, Siberian Branch of the Russian Academy of Sciences, Ul. Neftezavodskaya 54, Omsk 644040 (Russia)

E-mail: ktr@ihcp.oscsbras.ru

Abstract

The effect of chemical composition on the formation of the crystal structure and texture characteristics of the oxide system B_2O_3–Al_2O_3 obtained through impregnation of pseudoboehmite with the solutions of *ortho*-boric acid was studied. It was shown that the modification with boron oxide slows down the crystallization of aluminium oxide. According to the high-resolution TEM data, borate-containing aluminium oxides are composed of amorphous and crystalline primary particles. It was established by means of ^{27}Al MAS NMR and ^{11}B MAS NMR that aluminium atoms in the samples occur in octahedral, tetrahedral and penta-coordination, while boron atoms occur in trigonal and tetrahedral coordinations; their relative content depends on chemical composition. The dependence of the specific surface of B_2O_3–Al_2O_3 system on its composition has an extremal character; the maximum is achieved with B_2O_3 content 5 mass %.

Key words: borate-containing aluminium oxide, phase composition, texture, coordination state of aluminium

INTRODUCTION

At present, the systems based on anion-modified aluminium oxide have won broad application as acid catalysts and supports of catalysts. The introduction of the oxygenated compounds of sulphur, silicon, phosphorus, boron, and halogenated compounds into aluminium oxide allows one to control its structural and surface properties, as well as the dispersity and activity of the supported component. The advantages of the system B_2O_3–Al_2O_3 in comparison with other anion-containing aluminium oxides include the simplicity of synthesis and high stability due to which this material may be used in industrial processes with oxidative regeneration of the catalyst [1].

The use of borate-containing aluminium oxide as a catalyst for acid-controlled reactions and as acid support for bifunctional catalysts is known. In particular, the system B_2O_3–Al_2O_3 was studied as a catalyst of toluene disproportionation [2], alkene isomerization [2, 3], butene oligomerization [4, 5], Beckmann rearrangement [6], alcohol dehydration [2, 7], and incomplete oxidation of ethane [8]. In addition, this mixed oxide is used as a support for Ni and Re in the catalysts of oligomerization and metathesis [9, 10], Co–Mo [11] and Ni–Mo [12] in the catalysts of hydrofining, Pt in the catalysts of cyclohexene hydrogenation [13] and hydrodeoxygenation of plant oil [10], Ru in the catalysts of CO hydrogenation.

The properties of the B_2O_3–Al_2O_3 system are determined by its chemical composition and preparation method. The most widespread methods of the synthesis of this system are impregnation of aluminium oxide support with aqueous or methanol solutions of *ortho*-boric acid [3–5, 9, 11, 12], co-precipitation with ammonium hydroxide from aluminium nitrate and boric acid [2, 13], and sol-gel procedure [14–16] including the use of structure-forming additives [7]. Methods based on gas-phase deposition of boron oxide from ethyl borate [17] and low-temperature thermal decomposition of a mixture of aluminium nitrate and boric acid with organic additive [18] are also known.

The goal of the present work was to study the effect of the chemical composition and synthesis parameters of the $B_2O_3-Al_2O_3$ system prepared by impregnation of pseudoboehmite with the solutions of boric acid on the regularities of its formation and physicochemical properties.

EXPERIMENTAL

Initial compounds for the synthesis were commercially available pseudoboehmite (Industrial Catalysis JSC, Ryazan, Russia) and boric acid of kh. ch. reagent grade. Aluminium hydroxide with the humidity of 70−80 mass % was treated with the aqueous solutions of boric acid at a temperature of 90 °C. Then free water was evaporated at 90 °C, the samples were dried at 120 °C for 12 h annealed at 550 °C for 16 h. The solutions of orthoboric acid with different concentrations were used to vary boron oxide content in the catalysts.

The chemical composition of the samples was determined by means of optical emission spectroscopy with inductively coupled plasma (ICP-OES) using a Varian 710-ES atomic emission spectrometer with inductively coupled plasma.

The gravimetric and differential thermal analysis of dried samples (120 °C) was carried out with the help of a DTG-60 instrument of Shimadzu Co. within temperature range 20−1000 °C in the atmosphere of air at the heating rate of 10 °C/min.

The phase composition of the samples was determined with a Bruker D8 Advance diffractometer (CuK_α radiation). Annealed samples were scanned within the angle range $2\theta = 5-80°$ with the step of 0.1° and accumulation time 7 s in each point.

The dried samples (initial aluminium hydroxide and containing boric acid) were studied by means of thermal X-ray imaging using the same diffractometer, in the HTK 16 chamber (Anton Paar) with Pt−Rh heater. Heating rate was 5 °C/min, exposure before recording each diffraction pattern was 15 min. The following temperature steps were chosen (°C): 30, 150, 250, 300, 350, 400, 450, 500, 600, 700, 800. Determination of the coherent length was carried out according to Selyakov−Scherrer equation.

The electron microscopic studies of the samples were carried out using a JEM-210 JEOL electron transmission microscope (accelerating voltage 200 kV, resolution over the lattice 0.145 nm).

The ^{27}Al and ^{11}B NMR spectra of borate-containing aluminium oxides were recorded with an Avance-400 Bruker NMR spectrometer under the conditions of sample rotation at the magic angle (MAS) at a rate of 15 kHz in a zirconium rotor (4 mm in diameter). ^{27}Al NMR spectra were recorded at the frequency of 104 MHz, pulse duration was 25 µs, relaxation delay 0.5 s, chemical shift reference was the aqueous solution of 1 M $AlCl_3$. ^{11}B NMR spectra were recorded at the frequency of 128 MHz, pulse duration was 10 µs, relaxation delay 0.5 s, reference $BF_3[O(C_2H_5)_2]$.

The texture characteristics of the supports were determined from the analysis of nitrogen adsorption-desorption isotherms at 77.4 K recorded using the Micromeritics' ASAP-2020 M analyzer. Calculations of specific surface were carried out according to BET procedure within the relative pressure range $P/P_0 = 0.05-0.25$. Adsorption pore volume (V_{ads}) was determined from the value of nitrogen adsorption at $P/P_0 = 0.990$. Average pore diameter was estimated using equation $D = 4V_{ads}/S_{BET}$. The curves of pore size distribution (CPSD) were calculated by means of BJH from the adsorption branch.

RESULTS AND DISCUSSION

It is known [14, 16] that boron oxide may evaporate during the thermal treatment of $B_2O_3-Al_2O_3$ samples, so its actual content in the samples may be substantially lower than the calculated value. Below we present the data on the nominal and actual B_2O_3 content in samples (mass %):

Nominal	Actual
0	0
2	2.0±0.1
5	4.6±0.4
10	9.7±0.1
15	13.6±0.3
20	18.8±0.3
30	31.4±0.5

One can see that the actual composition coincides with the calculated one for the materi-
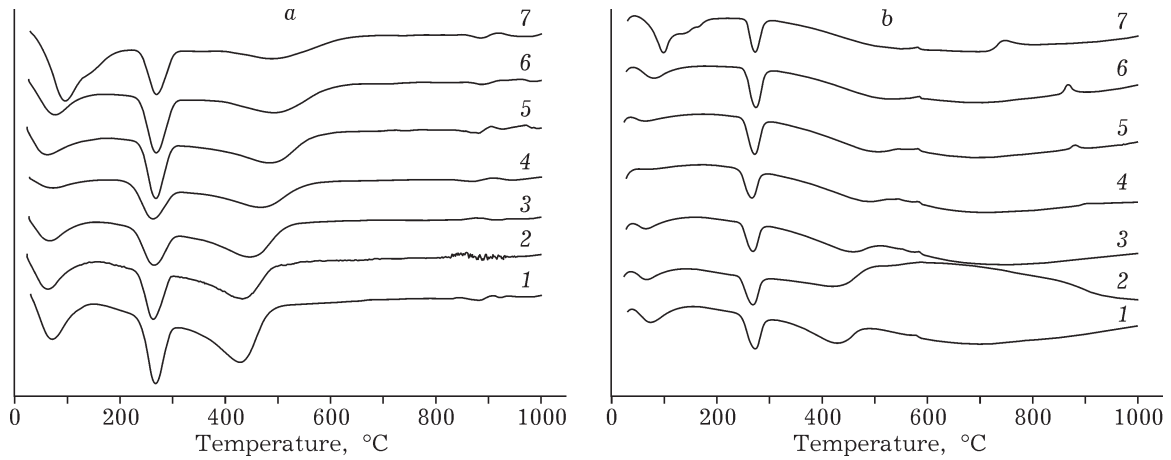
Fig. 1. DTG (*a*) and DTA (*b*) profiles of dried samples with different B$_2$O$_3$ content (mass %): 0 (AlOOH) (*1*), 2 (*2*), 5 (*3*), 10 (*4*), 15 (*5*), 20 (*6*), 30 (*7*).
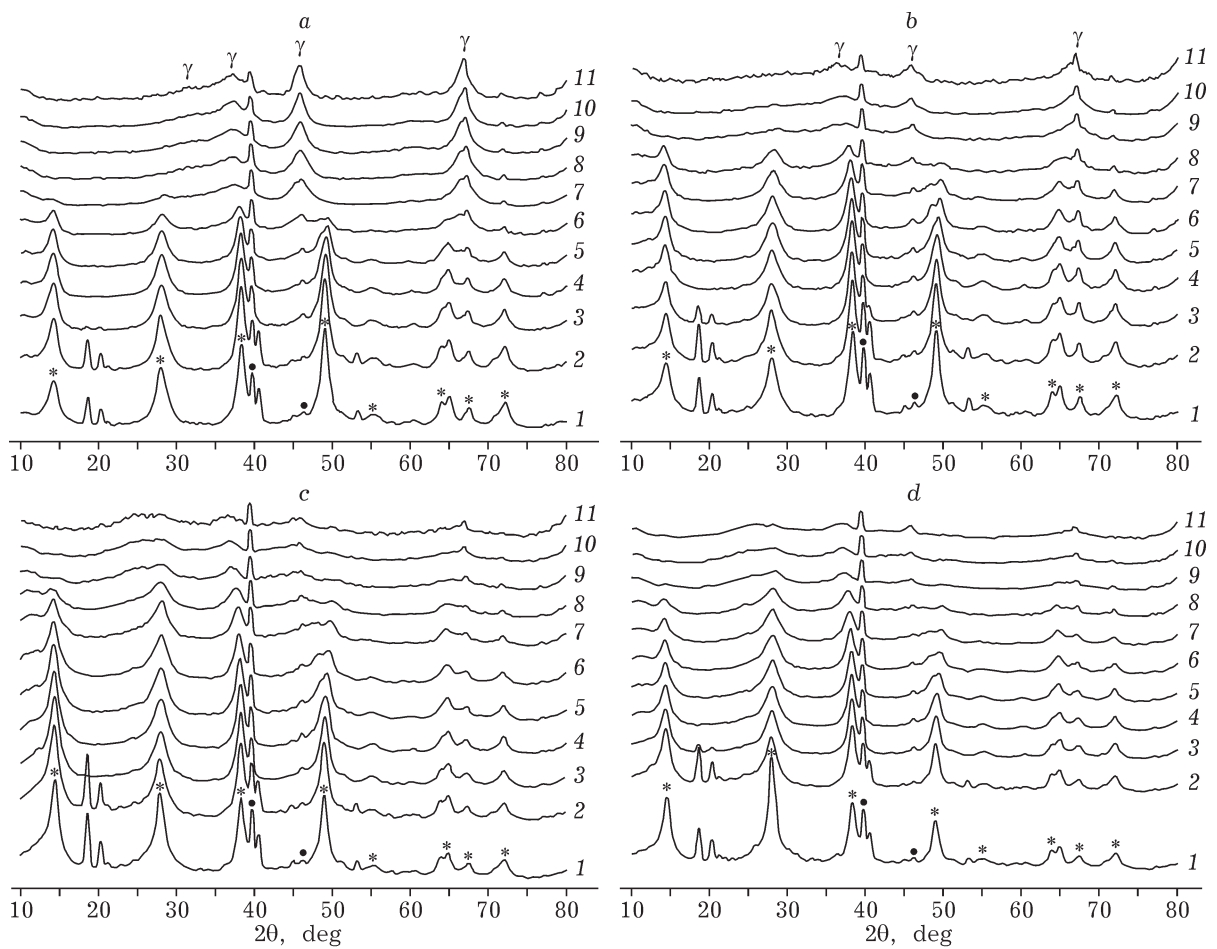
∗ Pseudoboehmite
• Platinum from the heater in thermal chamber
γ γ-Al$_2$O$_3$

Fig. 2. Diffraction patterns of the supports with different B$_2$O$_3$ concentrations (%): *a* − 0 (initial AlOOH), *b* − 10, *c* − 20, *d* − 30; process temperature (°C): 30 (*1*), 150 (*2*), 250 (*3*), 300 (*4*), 350 (*5*), 400 (*6*), 450 (*7*), 500 (*8*), 600 (*9*), 700 (*10*), 800 (*11*).

als with the mass concentration of B_2O_3 below 10 %. Small losses of boron oxide (not less than 1.5 mass %) are observed only when its concentration is 10−20 mass %. Therefore, the procedure involving evaporation at 90 °C allows us to avoid substantial losses of boron oxide during thermal treatment.

Three regions of mass loss may be distinguished in the thermogravimetric profiles of the samples under investigation (Fig. 1, *a*). Within temperature range 30−200 °C, physically adsorbed water is removed. For the sample containing 30 mass % boron oxide, also a peak connected with the decomposition of free boric acid is observed in this region. Within the range 240−300 °C, the DTG curves of all the samples exhibit a peak corresponding to dehydration of pseudoboehmite. The peak within the range 350−550 °C on DTG and DTA curves (see Fig. 1, *b*) is connected with crystallization of γ-Al_2O_3. With an increase in boron oxide content, broadening of this peak is observed, accompanied by a decrease in its intensity. Its extremal point on DTA curves shifts gradually from 430 °C for pure pseudoboehmite to 490 °C for the sample containing 30 mass % B_2O_3. So, the introduction of boron oxide into aluminium oxide hinders crystallization of the latter.

In addition to the mentioned peaks related to different stages of the formation of γ-Al_2O_3 crystal structure, within the range 740−910 °C the DTA curves of samples with 10 mass % and higher concentration of B_2O_3 contain an exo effect which is not accompanied by mass change. It is connected with the formation of crystal aluminoborate with the composition $2Al_2O_3 \cdot B_2O_3$ [2]. With an increase in B_2O_3 content in the system, the intensity of this peak increases, while it shifts to lower temperature region.

X-ray phase analysis of the dried samples in the mode of thermal X-ray imaging showed (Fig. 2) that the reflections characteristic of γ-Al_2O_3 appear at a temperature as low as 400 °C when a sample containing no B_2O_3 is heated in the chamber. The introduction of B_2O_3 in the amount of 10 mass % into the sample leads to an increase in the temperature of the start of crystallization of the aluminium oxide phase to 500 °C, while with higher concentration of the modifier the reflections related to the aluminium oxide phase do not appear in the diffraction patterns of the samples under study even at treatment temperature 600−800 °C. The coherent length was determined from thermal X-ray imaging for γ-Al_2O_3 in the samples containing 0−15 mass % boron oxide (Fig. 3). One can see that the coherent length of γ-Al_2O_3 for samples treated at the same temperature decreases with an increase in boron content of the samples. These data are in good agreement with DTA results of the samples and confirm that the addition of B_2O_3 into aluminium oxi-de hinders its crystallization. This is also evidenced by the results of XPA of the samples with different B_2O_3 content, annealed at a temperature of 550 °C for 16 h (Fig. 4). The integral intensity of reflections characteristic of γ-Al_2O_3
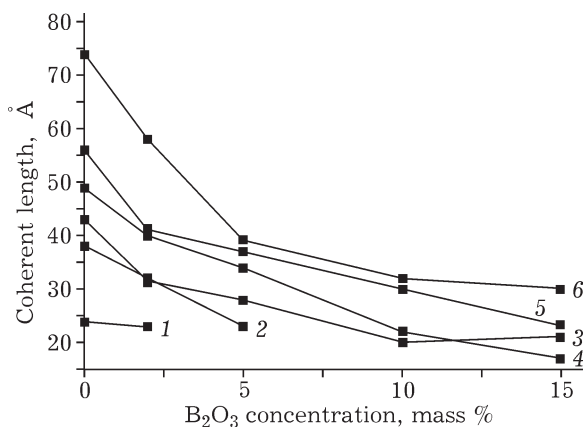
Fig. 3. Changes in the coherent length of aluminium oxide depending on B_2O_3 concentration at process temperature (°C): 400 (*1*), 450 (*2*), 500 (*3*), 600 (*4*), 700 (*5*), 800 (*6*).
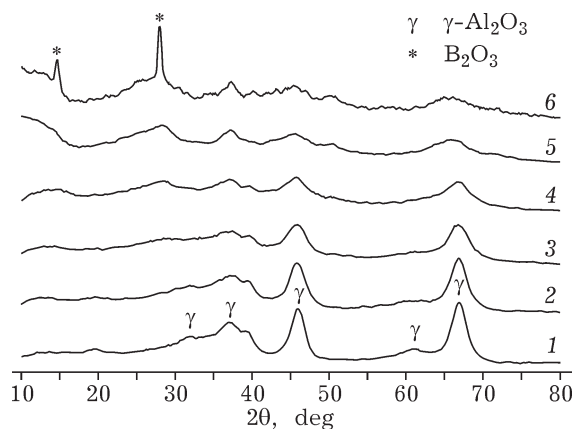
Fig. 4. Diffraction patterns of the samples of borate-containing aluminium oxide (550 °C). B_2O_3 concentration (mass %): 2 (*1*), 5 (*2*), 10 (*3*), 15 (*4*), 20 (*5*), 30 (*6*).
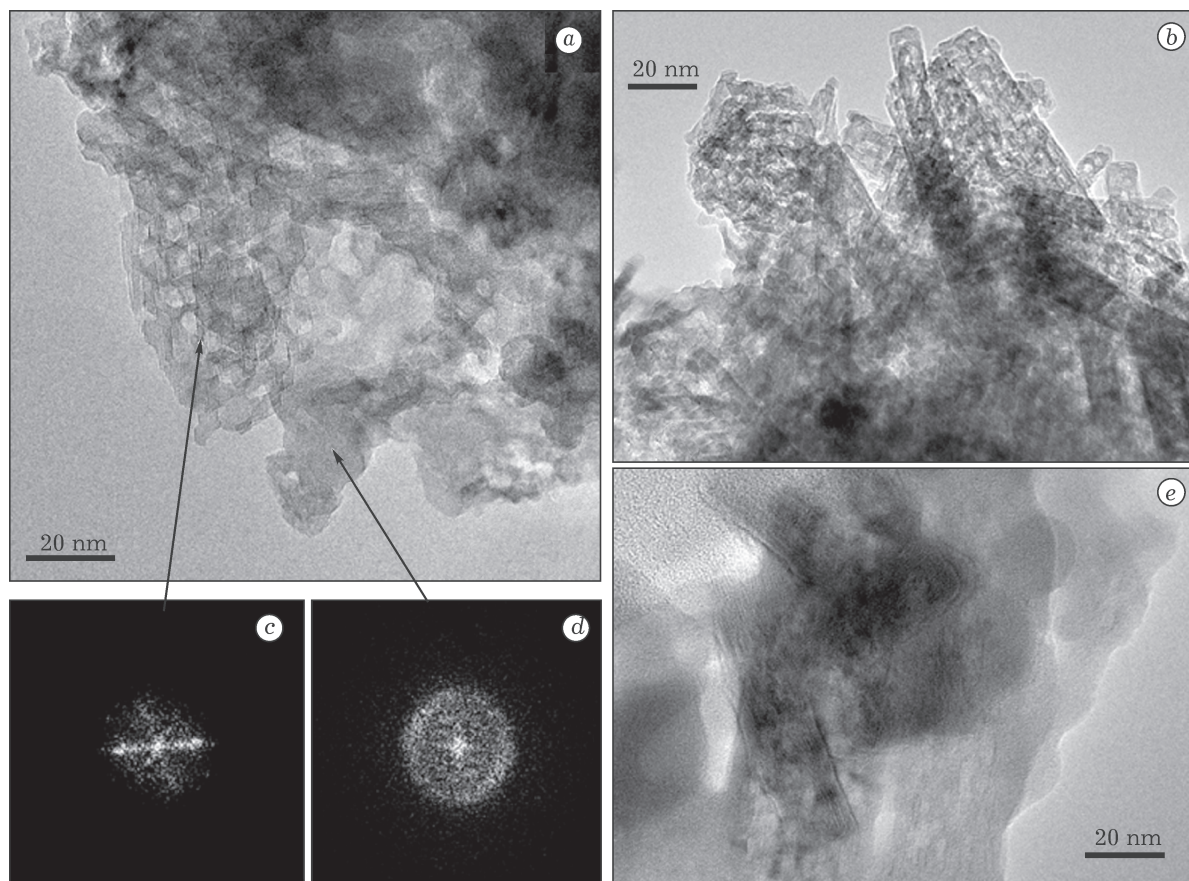
Fig. 5. Electron microscopic images of the samples (550 °C) with different B_2O_3 concentrations (mass %): 20 (*a*), 5 (*b*), 30 (*e*); *c*, *d* − electron diffraction patterns with Fourier transform for the crystalline and amorphous phases, respectively.

also decreases in the diffraction patterns of these materials with an increase in the concentration of boron oxide in them, and they are observed only as a halo for the samples with the mass concentration of B_2O_3 20 mass % and more.

The presence of aluminoborate phases in the samples under study could not be recorded unambiguously from XPA data. The diffraction patterns of the materials obtained in thermal chamber, with boron oxide 20 mass % and above (see Fig. 2) a halo is observed within the angle range $2\theta = 20-30°$. This effect can be connected with the crystallization of either aluminoborate phase or free boron oxide for which the most intense reflections are observed in this angle region. The reflections of the crystal phase of boron oxide are observed in the room-temperature diffraction pattern of the sample with the mass concentration of B_2O_3 30 % annealed at a temperature of 550 °C of 16 h.

According to the data of high-resolution transmission electron microscopy (HRTEM), the sample containing 5 mass % B_2O_3 (Fig. 5, *b*) is composed of the aggregates of needle-like or irregular shape formed by lamellar crystallites (3−5 nm) corresponding in morphology to γ-Al_2O_3 particles. The lattice parameters determined from Fourier electron diffraction patterns are 0.197 and 0.240 nm, which is characteristic of the interplanar spacings of γ-Al_2O_3 with indices (400) and (311), respectively. In the sample with the mass concentration of boron oxide 20 % (see Fig. 5, *a*) along with the crystal phase similar in its morphology to the above-described sample we observe the particles with amorphous structure, their size is 5 nm and more. The electron diffraction patterns of these particles have the appearance of diffuse rings, which is characteristic of the amorphous state. The sample containing 30 mass % B_2O_3 is represented by the crystallites without clear facing, surrounded by the amorphous phase (see Fig. 5, *e*). In the case of the samples with the mass concentration of B_2O_3 20 and 30 %, the
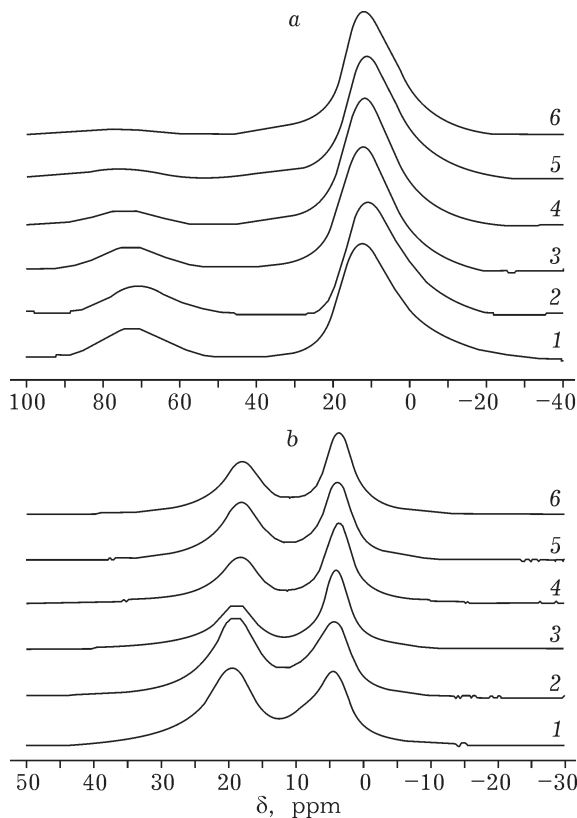
Fig. 6. ^{27}Al (*a*) and ^{11}B (*b*) MAS NMR spectra of the samples of borate-containing aluminium oxide (550 °C). B$_2$O$_3$ concentration (mass %): 2 (*1*), 5 (*2*), 10 (*3*), 15 (*4*), 20 (*5*), 30 (*6*).

high-resolution photographs exhibit the lattice planes with periodicity 0.136, 0.194, 0.236 and 0.264 nm (±0.005 nm). These interplanar spacings are observed either for aluminium and boron oxides or for aluminoborate compounds.

The ^{27}Al MAS NMR spectra of dried samples, independently of the concentration of boron oxide introduced, contain only one resonance in the region of 10 ppm, which corresponds to Al atoms in the octahedral coordination in pseudoboehmite. Therefore, the introduction of borate ions does not affect the volume structure of aluminium hydroxide at this stage of preparation, and the particles of the boron-containing phase are most likely dispersed on the surface of pseudoboehmite crystals.

Annealing of borate-containing samples leads to the appearance in their ^{27}Al MAS NMR spectra (Fig. 6, *a*) of the signals from Al atom in tetrahedral and octahedral coordination (chemical shift about 70 and 10 ppm, respectively), which is characteristic of γ-Al$_2$O$_3$. Integration of the corresponding peaks after their

decomposition shows (Table 1) that the relations between aluminium forms in the samples with different B$_2$O$_3$ content varies, while the fraction of tetrahedral atoms decreases from 21 to 3 % with an increase in the mass concentration of boron oxide from 2 to 30 %. According to the data reported in [2, 14], a decrease in the fraction of tetrahedral aluminium atoms is connected with the substitution of AlO$_4^{3-}$ ions by BO$_4^{3-}$ in the structure of the oxide, and the transition of a part of aluminium into the penta-coordinated state. The presence of penta-coordinated aluminium atoms in the system under study manifests itself as a low-intensity resonance in the region of 40 ppm. The fraction of these atoms in the sample containing 10 mass % boron oxide is 0.5 %, while for higher concentration of the modifying agent it increases to 3–4 %. It should be noted that there are low-frequency tails of the signals of aluminium atoms in the tetrahedral and octahedral coordinations. This may be the evidence of some disordering in Al$_2$O$_3$ structure.

The ^{11}B MAS NMR spectra of both the dried and annealed samples (see Fig. 6, *b*) contain two well resolved resonances with chemical shifts ~18 and ~3 ppm, related to boron atoms in the trigonal and tetrahedral coordination, respectively. The quantitative estimation of the relations between different forms of boron carried out by means of integration of the corresponding peaks (see Table 1), shows

TABLE 1

Ratio of aluminium and boron atoms in different coordinations in the samples of borate-containing aluminium oxide

Concentration of B$_2$O$_3$, mass %	Relative concentrations of atoms, %				
	Al			B	
	O	T	P	T	Tr
2	79	21	–	39	61
5	81	19	–	40	60
10	85	14	0.5	53	47
15	87	10	3	54	46
20	89	8	3	49	51
30	93	3	4	52	48

Notes. 1. O – octahedral, T – tetrahedral, P – pentahedral, Tr – trigonal coordination. 2. Dash – absent.

TABLE 2

Texture characteristics of the samples of borate-containing aluminium oxide

B_2O_3 concentration, mass %	S_{sp}, m^2/g	V_{por}, cm^3/g	D_m, nm
0	219	0.54	9.9
2	254	0.56	8.8
5	292	0.59	8.1
10	257	0.55	8.6
15	228	0.51	9.0
20	210	0.47	8.9
30	168	0.40	9.5

that the fraction of boron atoms in tetrahedral coordination increases with an increase in boron oxide concentration in the system to 15 mass %l it remains almost unchanged for higher B_2O_3 concentration.

The isotherms of nitrogen adsorption on aluminoborate supports correspond to the IV type of isotherms according to IUPAC classification; they are characterized by the presence of capillary condensation hysteresis and are typical for mesoporous materials [19].

The texture characteristics of annealed samples are shown in Table 2. The dependence of specific surface of the samples under study has the extremal appearance; the maximal value is observed for the sample containing 5 mass % B_2O_3. Specific pore volume for the samples with boron oxide concentration up to 15 % is practically the same, while with further increase in B_2O_3 concentration it decreases by 15−20 %. Lower values of S_{sp} and V_{por} parameters for the sample with the mass concentration of B_2O_3 30 % are connected with the presence of free unreacted boron oxide on its surface.

For aluminium oxide, the curves of pore size distribution exhibit a broad distribution within the range 3−40 nm with the maxima for the average pore diameters 4.2 and 8.1 nm. An increase in the concentration of boron oxide to 5 mass % leads to mesopore size distribution within the same range but with one maximum (6.0 nm) on the curves. With further increase in the concentration of B_2O_3, only some decrease in the intensity of peaks occurs, along with insignificant shift of the maximum to smaller pores without redistribution of mesopores over the size.

CONCLUSIONS

1. It is demonstrated that the method of synthesis of oxide systems $B_2O_3 - Al_2O_3$ used in the present work, relying on pseudoboehmite treatment with the aqueous solutions of orthoboric acid, followed by evaporation, drying and annealing, allows obtaining the materials with developed texture ($S_{sp} = 170-290$ m^2/g, $V_{por} = 0.40-0.59$ cm^3/g). This synthesis method is easier in comparison with the conventional co-precipitation method and does not lead to a decrease in specific surface and pore volume within a broad range of the concentrations of modifying additive, unlike for impregnation of aluminium oxides. In addition, this method allows one to avoid the losses of boron oxide at the stage of evaporation, which often happens during the preparation of borate-containing catalysts.

2. According to the data of thermogravimetry and X-ray phase analysis, the introduction of boron oxide into pseudoboehmite hinders crystallization of aluminium oxide from it during thermal treatment, while the introduction of the modifying agent in the amount of 15 mass % and more promotes the formation of X-ray amorphous material. In this situation, according to the data of HRTEM, the obtained X-ray amorphous borate-containing aluminium oxides are composed of amorphous and crystalline primary particles.

3. It was established by means of MAS NME that an increase in the concentration of B_2O_3 in the samples causes a decrease in the fraction of aluminium atoms in tetrahedral coordination and an increase in the fraction of penta-coordinated aluminium atoms and boron atoms in the tetrahedral coordination.

REFERENCES

1 Lamberov A. A., Sitnikova E. Yu. Gilmnov R. R., Sidorov N. A., *Katal. Prom.,* 3 (2010) 55.
2 Peil K. P., Galya L. G., Marcelin G., *J. Catal.,* 115, 2 (1989) 441.
3 Bautista F. M., Campelo J. M., Garcia A., Luna D., Marinas J. M., Moreno M. C., Romero A. A., Navio J. A., Maciasy M., *J. Catal.,* 173, 2 (1998) 333.
4 Lavrenov A. V., Duplyakin V. K., *Kinet Katal.,* 50, 2 (2009) 249.
5 Flego C., Parker Jr. W., *Appl. Catal. A: Gen.,* 185, 1 (1999) 137.

6 Curtin T., McMonagle J. B., Ruwet M., Hodnett B. K., *J. Catal.*, 142, 1 (1993) 172.

7 Xui T., Wang J., Liu Q., *Micropor. Mesopor. Mater.*, 143, 2−3 (2011) 362.

8 Colorio G., Vedrine J. C., Auroux A., Bonnetot B., *Appl. Catal. A: Gen.*, 137, 1 (1996) 55.

9 Sibeijn M., Vanveen J. A. R., Bliek A., Moulijn J. A., *J. Catal.*, 145, 2 (1994) 416.

10 Lavrenov A. V., Buluchevskii E. A., Karpova T. R., Moiseenko M. A., Mikhailova M. S., Chumachenko Yu. A., Skorplyuk A. A., Gulyaeva T. I., Arbuzov A. B., Leontyeva N. N., Drozdov V. A., *Chem. Sustain. Dev.*, 19, 1 (2011) 87.
URL: http://www.sibran.ru/en/journals/KhuR

11 Rinaldi N., Usman, Al-Dalama K., Kubota T., Okamoto Y., *Appl. Catal. A: Gen.*, 360, 1 (2009) 130.

12 Torres-Mancera P., Ramнrez J., Cuevas R., Gutiérrez-Alejandre A., Murrieta F., Luna R., *Catal. Today*, 107−108 (2005) 551.

13 Chen Y.-W., Li C., *Catal. Lett.*, 13, 4 (1992) 359.

14 Forni L., Fornasari G., Tosi C., Trifro F., Vaccari A., Dumeignil F., Grimblot J., *Appl. Catal. A: Gen.*, 248, 1−2 (2003) 47.

15 Chen T. D., Wang L., Chen H. R., Shi J. L., *Mater. Lett.*, 50, 5−6 (2001) 353.

16 Dumeignil F., Rigole M., Guelton M., Grimblot J., *Chem. Mater.*, 17, 9 (2005) 2369.

17 Sato S., Hasebe H., Sakurai H., Urabe K., Izumi Y., *Appl. Catal.*, 29, 1 (1987) 107.

18 Simon S., Vander Pol A., Reijerse E. J., Kentgens A. P. M., van Moorsel G. J., De Boer E., *J. Chem. Soc., Faraday Trans.*, 90, 18 (1994) 2663.

19 Keltsev N. V., Osnovy Adsorbtsionnoy Tekhniki, Khimiya, Moscow, 1984, p. 29.